Original research

Deep exploration of a *CDKN1C* mutation causing a mixture of Beckwith-Wiedemann and IMAGe syndromes revealed a novel transcript associated with developmental delay

Siren Berland ,[1] Bjørn Ivar Haukanes,[1] Petur Benedikt Juliusson,[2,3] Gunnar Houge[1]

► Additional material is published online only. To view, please visit the journal online (http://dx.doi.org/10.1136/jmedgenet-2020-107401).

[1]Department of Medical Genetics, Haukeland University Hospital, Bergen, Norway
[2]Department of Clinical Science, University of Bergen, Bergen, Hordaland, Norway
[3]Department of Paediatrics, Haukeland University Hospital, Bergen, Norway

Correspondence to
Dr Siren Berland, Department of Medical Genetics, Haukeland University Hospital, Bergen 5021, Norway;
siren.berland@helse-bergen.no

Received 18 August 2020
Revised 20 November 2020
Accepted 28 November 2020
Published Online First 21 December 2020

To cite: Berland S, Haukanes BI, Juliusson PB, *et al*. *J Med Genet* 2022;**59**:155–164.

ABSTRACT

Background Loss-of-function mutations in *CDKN1C* cause overgrowth, that is, Beckwith-Wiedemann syndrome (BWS), while gain-of-function variants in the gene's PCNA binding motif cause a growth-restricted condition called IMAGe syndrome. We report on a boy with a remarkable mixture of both syndromes, with developmental delay and microcephaly as additional features.

Methods Whole-exome DNA sequencing and ultra-deep RNA sequencing of leucocyte-derived and fibroblast-derived mRNA were performed in the family.

Results We found a maternally inherited variant in the IMAGe hotspot region: NM_000076.2(*CDKN1C*) c.822_826delinsGAGCTG. The asymptomatic mother had inherited this variant from her mosaic father with mild BWS features. This delins caused tissue-specific frameshifting resulting in at least three novel mRNA transcripts in the boy. First, a splice product causing CDKN1C truncation was the likely cause of BWS. Second, an alternative splice product in fibroblasts encoded IMAGe-associated amino acid substitutions. Third, we speculate that developmental delay is caused by a change in the alternative *CDKN1C-201* (ENST00000380725.1) transcript, encoding a novel isoform we call D (UniProtKB: A6NK88). Isoform D is distinguished from isoforms A and B by alternative splicing within exon 1 that changes the reading frame of the last coding exon. Remarkably, this delins changed the reading frame back to the isoform A/B type, resulting in a hybrid D–A/B isoform.

Conclusion Three different cell-type-dependent RNA products can explain the co-occurrence of both BWS and IMAGe features in the boy. Possibly, brain expression of hybrid isoform D–A/B is the cause of developmental delay and microcephaly, a phenotypic feature not previously reported in *CDKN1C* patients.

INTRODUCTION

The imprinted and predominantly maternally expressed cell cycle inhibitor *CDKN1C* located to 11p15.5 encodes a negative growth regulator also called $p57^{Kip2}$. This gene is associated with two contrasting phenotypes: the overgrowth disorder Beckwith-Wiedemann syndrome (BWS [MIM:130650]) and the growth-restricted IMAGe syndrome ([MIM:614732], an acronym for Intrauterine growth restriction, Metaphyseal dysplasia, Adrenal insufficiency and Genital abnormalities).[1] IMAGe and rare cases of Silver-Russel syndrome (SRS) are caused by gain-of-function (GoF) mutations in the PCNA-binding motif of CDKN1C, while loss-of-function (LoF) mutations are found in 8% of BWS cases.[2–4]

CDKN1C is a cyclin-dependent kinase inhibitor (CDI) belonging to the CIP/Kip family and encoded by a small gene with three to four exons of which two to three are protein coding. Other members are $p21^{Cip1}$ (CDKN1A) and $p27^{Kip1}$ (CDKN1B), which inhibit cell growth in G1 and can cause cell-cycle arrest. The ENSEMBL database (ensembl.org) contains several *CDKN1C* transcripts encoding different isoforms; *CDKN1C-202* encodes the 316aa isoform A, *CDKN1C-203* encodes an alternative isoform A with different UTRs, *CDKN1C-204* encodes the 305aa isoform B with an alternative start site and *CDKN1C-201* encodes the 131aa A6NK88 isoform that we call isoform D (see figure 1). CDKN1C has an N-terminal CDI (cyclin-dependent kinase inhibitor) domain, a central PAPA (proline-alanine) repeat and C-terminally the PCNA (proliferating cell nuclear antigen)–binding motif and an overlapping putative KRKR-containing nuclear localisation signal.

BWS is most often caused by sporadic loss-of-methylation (LoM) of imprinting centre 2 (IC2) on the maternal chromosome 11 that results in diminished *CDKN1C* expression, found in about 50%–60% of BWS, followed by paternal segmental uniparental disomy (UPD) 11p also involving the paternally methylated imprinting centre 1 (IC1) of the IGF2-H19 domain in about 20%.[5] IC1 gain-of-methylation (GoM) has been reported in 5%–10% of the patients, whereas microdeletions of IC1 and *CDKN1C* variants are important causes of familial BWS. Other chromosomal CNVs, balanced rearrangements, multilocus imprinting disturbances and mosaic genome-wide paternal UPD are rare causes of BWS. Typical features are omphalocele/umbilical hernia, macroglossia, neonatal hyperinsulinism, Wilms tumour, lateralised overgrowth, macrosomia, ear creases and pits, large internal organs, adrenal fetal cortex cytomegaly and renal abnormalities.[5 6] Genotype–phenotype correlations are reported as *CDKN1C* mutations have higher rates

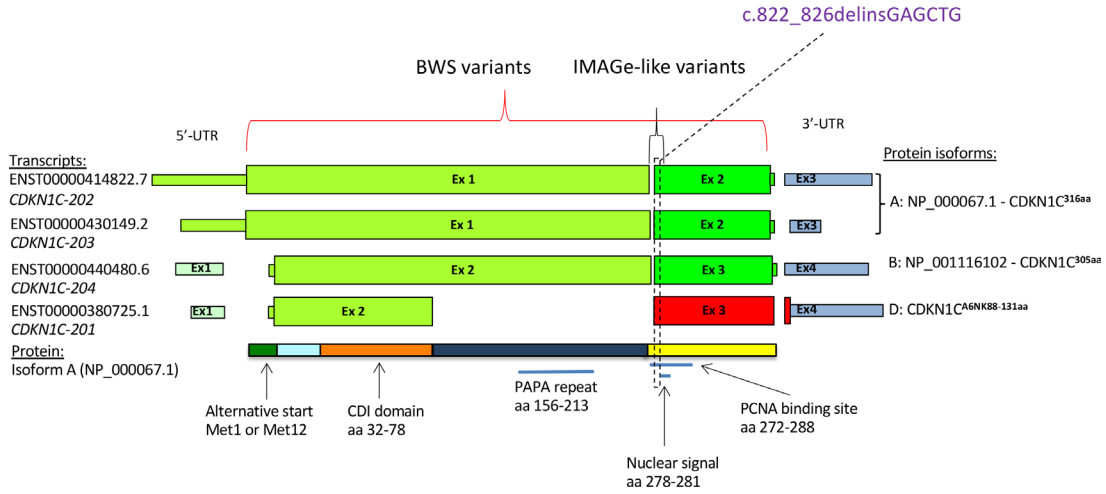

Figure 1 Overview of *CDKN1C* transcripts according to ENSEMBL GRCh38.p11, and corresponding protein isoform A. Above, the localisation of the patient's delins variant (purple and open vertical box) and reported IMAGe and Beckwith-Wiedemann syndrome (BWS) mutations. The transcripts are not drawn to scale. The narrow bars represent untranslated regions (UTRs). To the left, ENSEMBL reference transcripts, to the right protein isoforms (NCBI protein reference sequences if known). Below, isoform A (316 aa, NP_000067.1) with amino acid borders, domains, motifs, repeats and their approximate localisation. The protein isoform A of 316 aa is encoded by two different transcripts (*CDKN1C-202* and *CDKN1C-203*) with different lengths of UTRs but encoding identical amino acids. Isoform B (305 aa) uses an alternative start methionine, 11 aa downstream. A6NK88 is the UniProtKB accession code for the 131 aa protein isoform that we call isoform D. *CDKN1C-206* (encoding isoform C) is not included in this figure as this transcript was not detected in our analysis.

of preterm birth, cleft palate, abdominal wall defect, capillary malformations and ear signs, while intrauterine overgrowth and tumours are less common.[7 8] *CDKN1C*-restricted BWS features are also reported, including maternal pre-eclampsia, genital abnormalities, polydactyly, polythelia and posterior fossa abnormalities.[7 9–12]

Maternally inherited GoF variants can cause IMAGe syndrome, an SRS-like phenotype,[13] and short stature with diabetes,[14] but such variants are rare causes of growth restriction.[15–17] IMAGe was first described in 1999[18] and linked to *CDKN1C* in 2012.[4] Besides, SRS phenotype with salt-wasting due to adrenal insufficiency mimicking IMAGe was described in two patients with 11p15 maternal duplications.[19] So far, only 12 molecularly confirmed IMAGe/SRS-like families are reported, and all variants but one which we consider to be of unknown significance (VUS),[17] are located in the PCNA-binding site.[4 13 14 20–25] Most studies suggest that IMAGe/SRS variants increase protein stability,[13 20 26] although not confirmed by Kerns *et al*.[14] The mechanism is not fully elucidated but might include impaired proteasome-mediated degradation.[20] Clinical findings include short stature, neonatal adrenal hypoplasia, hypercalciuria, metaphyseal dysplasia with delayed bone age, low-set and posteriorly rotated ears, frontal bossing and relative macrocephaly, and less frequently hearing loss and craniosynostosis.[27] A *Drosophila melanogaster* IMAGe model showed impaired eye and wing growth,[4] demonstrating that cdkn1c plays a role in cell proliferation in multicellular organisms. There are no consensus criteria for IMAGe syndrome, and metaphyseal dysplasia and adrenal hypoplasia are not present in all. So far *CDKN1C* has not been associated with a neurological phenotype in humans, but developmental delay is reported in a few patients with BWS with structural brain abnormalities.[7 11 27] Furthermore, a mixture of IMAGe and BWS has not been published before.

Here, we report on a boy heterozygous for a delins variant in *CDKN1C*, replacing five nucleotides with six others in the junction between exons 1 and 2 of the main isoform. This delins caused a mixture of IMAGe and BWS-like features, and possibly also developmental delay as no alternative causes for this were found. We aimed to determine how this complex variant could have both GoF and LoF effects and to find a potential explanation for the affected brain function. Our work revealed that a novel *CDKN1C* transcript with a non-canonical C-terminal reading frame encoding isoform A6NK88 (named isoform D by us) was also affected by the delins, and as isoform D is also expressed in the brain, this could be the cause of his developmental delay.

METHODS

The boy and his family were clinically examined, given genetic counselling and consented to RNA analysis to investigate the molecular consequences of the *CDKN1C* variant.

Sanger sequencing

We used *CDKN1C* reference sequence NM_000076.2 encoding a 316 aa protein (isoform A). Sequence pilot (JSI Medical Systems, Ettenheim, Germany) software was used for interpretation. DNA was isolated from peripheral blood obtained from the boy, his parents, his mother's siblings, maternal grandparents and maternal grandfather's parents, and sequenced. To explore the mosaic pattern in the maternal grandfather, we analysed additional DNA obtained from buccal swab, urine and fibroblasts from four distinct skin biopsies.

RNA isolation, sequencing of cDNA and qPCR

Total RNA was isolated from fibroblasts from biopsies of healthy skin (two biopsies from the boy, one from his mother and four from his grandfather), one epidermal nevus in the boy and also from blood samples (from the boy, both parents and the grandfather) by using the RNeasy Mini Kit (QIAGEN, Hilden, Germany) for fibroblasts and PAXgene Blood RNA Kit (QIAGEN) for blood samples. cDNA was synthesised following the manufacturer's protocol. The variant was amplified by

quantitative qRT-PCR using different primer sets taking alternative acceptor site usage into account and also spanning the variant affecting transcript ENST00000380725.1 *CDKN1C-201* (for a full list of transcripts, see figure 1). The primer sequences are given in online supplemental file. We examined expression levels of wt (wild type) and mutant (delins) *CDKN1C*, and wt *CDKN1C-201* by qRT-PCR on RNA isolated from both blood and cultured fibroblasts from the boy (all biopsies), his mother and grandfather (where we picked the biopsy with highest mutation load), and blood from his father. Primers and probes were from Applied Biosystems, Life Technologies, and assessment of B2M (beta-2-microglobulin) RNA (Applied Biosystems) served as endogenous controls. At least two runs per experiment were performed, and two different probes for both *CDKN1C-201* and mutant *CDKN1C* were analysed.

Total RNA deep sequencing

We used blood-derived RNA from the boy, his mother and grandfather, and an unrelated healthy adult female, and fibroblast RNA from the boy's skin biopsy #2. Whole transcriptome sequencing libraries were generated using the Illumina TruSeq Stranded Total RNA kit with Ribo-Zero Gold depletion for fibroblasts and Ribo-Zero Globin depletion for blood, according to the manufacturer's protocols. Libraries were quality checked on the Agilent Bioanalyzer system and accurately quantified using the KAPA qPCR quantification kit. Libraries were paired-end sequenced on the Illumina HiSeq4000 system with a read length of 2×75 nt. Sequencing was performed ultra-deep for all libraries (~250 million reads per sample). RNA-sequencing reads were aligned to the human genome reference (GRCh38) using HISAT2 (V.2.0.5).[28 29] Reads aligned within the coding part of the genome (adequate Gencode gtf annotation file) were counted using featureCounts.[30] To resolve alternative *CDKN1C* transcripts, we created supplementary reference files in FASTA format and realigned reads. Data were visualised in IGV (Integrative Genomics Viewer V.2.3.74) (online supplemental file). We only considered splice junction tracks (SJTs) when counting reads and manually checked all reads in a region of interest. All samples were run in the same flow cell.

Whole-exome sequencing

Whole-exome sequencing (WES) was performed on genomic DNA isolated from blood from the patient and parents. DNA samples were prepared using SeqCap EZ MedExome Target Enrichment Kit (Roche NimbleGen, Madison, WI) and followed by paired-end 150 nt sequencing on an Illumina NextSeq500. The paired-end reads were aligned using the Burrows-Wheeler Alignment tool and variant calling was performed using the Genome Analysis Toolkit (GATK; Broad Institute, Cambridge, MA) according to GATK's Best Practices guidelines. Mean #reads per base pair in the exome was 83X with 97.7% of the base pairs covered at least 10 times. Data annotation and interpretation were performed using the NGS module of Cartagenia Bench Lab software (Agilent, Santa Clara, CA).

CNV and methylation analysis

The boy's DNA isolated from peripheral blood and fibroblasts (two from normal skin and one benign nevus) was analysed for 11p15 CNVs and methylation aberrations by SALSA MS-MLPA Probemix ME030-C3 BWS/RSS (MRC-Holland, Amsterdam, NL). Also, DNA from blood was tested for other imprinted diseases using the SALSA MS-MLPA Probemix ME032-A1 UPD7-UPD14, and for genomic CNVs by CytoScanHD Array (Thermo Fisher Scientific, Waltham, MA).

Table 1 Clinical findings in the patient and possible associations to *CDKN1C*-related syndromes

Clinical features	BWS (score)	IMAGe (NH-CSS)	New
Polyhydramnios	X (1)		
Pre-eclampsia in mother	X		
Omphalocele	X (2)		
Large tongue	X (2)		
Neonatal hypoglycaemia	X (1)		
Neonatal apnoea	X		
Infraorbital crease	X		
Midface retrusion	X		
Long and grooved philtrum	X		
Nevus flammeus	X (1)		
Ear creases	X (1)		
Patent ductus arteriosus	X	X	
Inguinal hernia	X	X	
Cryptorchidism, bilateral	X	X	
Small testes		X	
Small for gestational age		X (1)	
Long gracile diaphysis		X	
Broad metaphysis		X	
Delayed bone age		X	
Bifrontal bossing		X	
Low set, posteriorly rotated ears		X	
Feeding difficulties		X (1)	
Broad nasal bridge and tip		X	
Hypotonia		X	
Small kidneys		?	X
Thin upper lip			X
Strabismus	?		X
Rib synostosis			X
Developmental delay			X
Microcephaly (postnatal)			X
Relative macrocephaly at birth		X (1)	

The number in parentheses are criteria score according to Beckwith-Wiedemann syndrome (BWS) clinical consensus score and Netchine-Harbison Clinical Silver-Russel Syndrome score (NH-CSS).[6 33]

Microsatellite analysis

To determine *CDKN1C* haplotypes and allele segregation, and to explore on which parental allele the grandfather's de novo variant arose, an informative haplotype was set up by simple tandem repeat markers amplified by PCR and size determined. There were two informative markers upstream and four downstream of *CDKN1C* (online supplemental file). The haplotype analysis was performed on DNA from peripheral blood from the patient, his parents, his mother's siblings, maternal grandparents and the grandfather's parents.

RESULTS

Clinical history and findings in the boy

Clinical findings in the patient are summarised in table 1 and illustrated in figure 2. Omphalocele was discovered by routine ultrasound in week 19 of gestation, amniocentesis was performed, and the pregnancy was complicated by maternal hyperemesis, pre-eclampsia, diabetes from week 29 and later polyhydramnios. He was born after caesarean section in gestation week 34+2

Figure 2 Boy at age 3 months (A, C, D), 6 months (B) and 27 months (G, F), with clinical features of both Beckwith-Wiedemann syndrome (ie, omphalocele, midface retrusion, large cheeks, hypertelorism with down-slanted palpebral fissures, infraorbital and ear creases, a fading glabellar capillary malformation, and a long and marked philtrum with a thin upper lip, wide mouth with a high palate and macroglossia) and IMAGe (slender habitus, feeding difficulties, frontal bossing, broad nasal bridge and a wide tip, low set and posteriorly rotated ears, long and slender finger and toes). Radiographs of leg (G) showing long and slender diaphysis and broad metaphysis, with a delayed bone age of fingers (F).

with birth weight 2160 g (−1.1 SDS), birth length 42 cm (−2.5 SDS) and head circumference 32 cm (0 SDS) (all measurements adjusted for prematurity). Placental weight was on the 90th percentile. Apgar score was 3/5/7 after 1, 5 and 10 min, respectively. He had mild hypoglycaemia (1.5 mmol/L) and compromised respiration. The giant omphalocele also contained liver tissue, and he underwent several surgeries before the abdominal wall finally was closed at 3 months of age. He suffered from apnoeic spells and needed CPAP until he was discharged from the hospital 5 months of age. He was exclusively fed by nasogastric tube for the first 5 months, and the tube was removed after 12 months. At the age of 3 years, he had been through more than 20 surgeries, including for patent ductus arteriosus, inguinal hernia and cryptorchidism. He had dysmorphic features as illustrated in figure 2, small intra-abdominal testes, multiple benign epidermal nevi and mild hypotonia. At follow-up at 25 months of age, his length was 0.8 SDS, weight −2.0 SDS and he was now microcephalic (−2.7 SDS). Motor milestones were delayed; he could sit at 15 months and walk without support at 2 years and 10 months of age. At age 3 years, he could speak a few simple words, and at age 5 years he had 3–4 words sentences with articulation problems. He had a normal neurological examination, hearing, vision and social development, but marked global delayed yet without formal assessment. He received speech, education and physical therapy. Cerebral MRI was normal, repeated abdominal ultrasounds from the age of 4 months showed small kidneys bilaterally and no organomegaly. At 2.5 years, an ACTH-stimulation test did not reveal adrenal insufficiency, and skeletal X-ray showed long and slender diaphyses, broad metaphyses, a fusion of left fourth and fifth ribs, and a 1.5-year delay in bone maturation. At age 5 years, his length was −1.5 SDS, head circumference centiles unchanged, confirming a postnatal/secondary microcephaly (−2.5 SDS), and he still had a low BMI of 12.9 (−2.8 SDS). He was scheduled to cancer surveillance every sixth month until 7–8 years of age.

Family history

The boy's phenotypically normal parents are non-consanguineous, the mother was 28 and the father 42 years at his birth. Clinical examination and birth history in the mother were negative for BWS features. Head circumferences were at 99th percentile (mother) and 60th percentile (father). The maternal grandfather was >5 kg at birth, and a large tongue was commented on neonatally, suggesting macroglossia. At examination at age 58 years, he was 181 cm tall with a wide mouth, slightly short halluces, no asymmetry, a normal skeletal X-ray survey and normal cognition.

Diagnostic workup

During pregnancy, a normal male karyotype 46,XY was found in amniotic fluid cells. After birth, clinical suspicion of BWS in the boy warranted MS-MLPA of the BWS region, which was normal in DNA from blood, skin and epidermal nevus. However, sequencing of *CDKN1C* verified BWS (see next section). Due to borderline short stature, developmental delay and postnatal microcephaly, further analyses were performed with normal results: high-resolution CNV analysis, UPD screening and trio-based WES.

Interpretation of the *CDKN1C* variant

Sanger sequencing of *CDKN1C* (NM_000076.2/ENST00000414822.7) revealed a heterozygous delins variant in the sequence encoding the PCNA binding motif affecting the

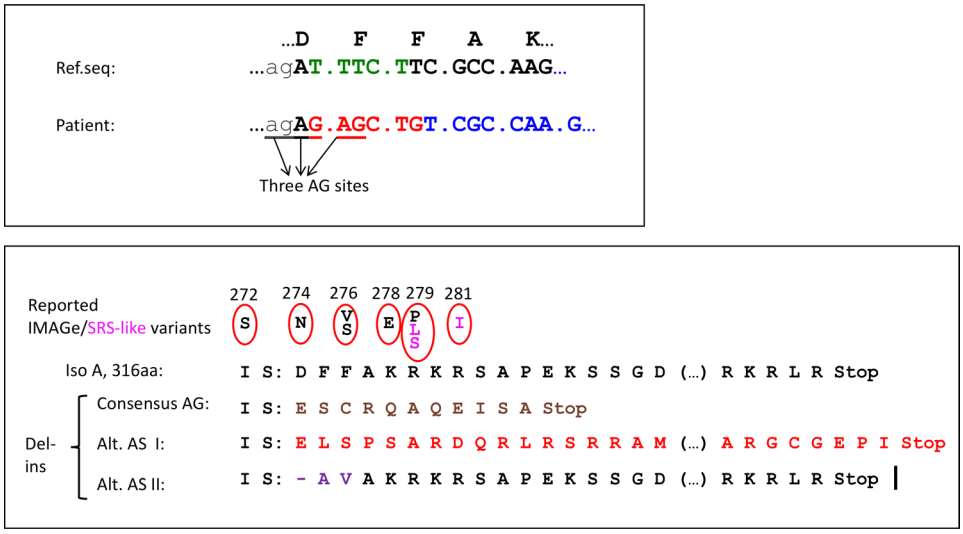

Figure 3 Predicted impact of the delins variant c.822_826delinsGAGCTG on DNA and isoform A. Upper panel shows the CDKN1C intron 2/exon 3 junction with reference amino acids on top and the reference nucleotide sequence (ENST00000414822.7, CDKN1C-202) just below. Intron sequences are written in lower case letters and exon sequences in capital letters. The five deleted nucleotides are in green. The bottom line shows the mutated sequence with the six inserted nucleotides in red, the three adjacent AGs (potential acceptor sites/AS) underlined and the out-of-frame sequence marked in blue. The lower panel shows details of the predicted amino acid sequence and changes introduced by the delins variant in amino acid numbers according to protein isoform A (316aa—NP_000067.1). On top reported IMAGe (black) and Silver-Russel syndrome (SRS)–like variants (magenta) from literature with the corresponding amino acid change, then the reference protein product, followed by the mutated products using the consensus AG (p.Asp274GlufsTer12), the protein product if alternative acceptor site I is used (p.Asp274GlufsTer47) and the protein product if alternative acceptor site II is used (p.Asp274_276delinsAlaVal). Parentheses (…) represent 21 amino acids omitted from the figure.

5′-end of exon 2: c.822_826delinsGAGCTG. The delins caused frameshifting and a premature termination codon (PTC) about 100 nucleotides upstream of the exon 2–3 junction. This change should either lead to nonsense-mediated mRNA decay (NMD) or synthesis of a truncated protein Asp274GlufsTer12, that is, an LoF change that fits with BWS phenotype. However, the delins also introduced two new putative splice junction AG acceptor sites, in addition to the consensus AG site (figure 3, upper panel). Use of alternative acceptor site I will also lead to a frameshift and a new stop codon, but in the very last protein-coding exon, that is, Asp274GlufsTer47, which should escape NMD (figure 3, lower panel). The corresponding protein product contains a modified C terminus including substitutions of four IMAGe-associated amino acids and introduce the known GoF variant Phe276Ser.[4] Use of alternative acceptor site II would be in line with the canonical reading frame of the protein's C-terminal part, but also include deletion of three and insertion of two new amino acids in the PCNA-binding motif: 274_276delinsAlaVal. This would modify one IMAGe residue (Asp274Ala), but also introduce a previously reported IMAGe-associated substitution: Phe276Val (figure 3).[4] This alternative transcript can be compared with known IMAGe-mutated transcripts, resulting in increased protein stability or affected PCNA binding.

The predicted out-of-frame C-terminal product from alternative acceptor site I, p.(Asp274GlufsTer47) (figures 3 and 4), was analysed by BLAST and found to be almost identical to *CDKN1C-201*, encoding a 131 amino acid isoform we call isoform D (UniProtKB accession A6NK88). Isoform D consists of the common CDI domain with a unique C-terminal D-tail, marked in red in figure 4, and its alternative splicing bypasses the PAPA-repeat region (figure 1). In addition to the PCNA-related amino acid substitution, the delins could also affect isoform D by introducing a frameshift that changed the reading frame back to the canonical reading frame (marked in yellow in figure 4). The predicted hybrid protein had elements from two distinct isoforms, D and A/B, where the D-type splicing causes direct connection of the CDI domain to an altered PCNA-binding motif, and where delins-induced frameshifting causes the C terminus to be of A/B type and not D type.

Diagnostic analysis of the family

The boy's asymptomatic mother was also heterozygous for the delins, compatible with a paternally imprinted allele in her, and further family studies including haplotype segregation analysis confirmed that the variant arose de novo on the grandfather's maternal allele. The mild BWS features in the grandfather indicated mosaicism, which was confirmed by DNA analyses of multiple tissues; only wt was present in fibroblasts from three out of four skin biopsies and a buccal swab, while the delins was found in blood, urine sediment and skin biopsy from the left leg. cDNA Sanger sequencing and qPCR cDNA sequencing confirmed the presence of both wt and (at a lower level) the delins allele in the boy, his mother and grandfather. Gene expression levels appeared generally low. Only in fibroblasts from the boy, the delins seemed to be more abundant than the wild-type transcript. Primers were also designed to cover the use of the two alternative splice acceptor sites illustrated in figure 3, but corresponding isoform-A/B-derived transcripts were not detected. However, sequencing demonstrated that wild-type isoform D (*CDKN1C-201*) transcript was present in blood from all family members and controls, and the delins-*CDKN1C-201* transcript was present in blood from the boy.

Semi-quantitative real time-PCR (qPCR) verified the presence of both *CDKN1C* (isoform A/B) and *CDKN1C-201* (isoform D) transcripts in blood samples from the patient, parents and grandfather. Also, isoform A/B was found in fibroblasts from all family members. Transcript levels were low compared with the B2M control and considerably lower in fibroblasts than in blood. Expression of delins-*CDKN1C* was seen in blood from

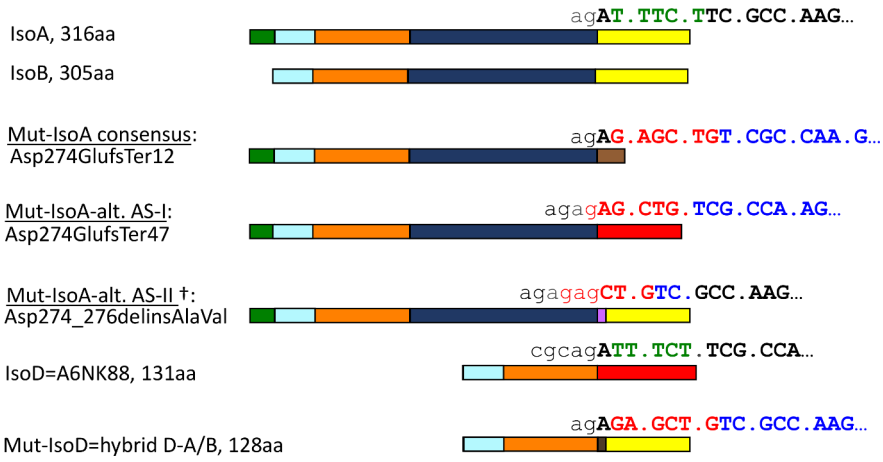

Figure 4 Overview of the predicted protein products. From top, wild-type isoform A (encoded by transcripts ENST00000414822.7=CDKN1C-202 and ENST00000430149.2=CDKN1C-203), wild-type isoform B (ENST00000440480.6=CDKN1C-204), followed by three predicted CDKN1C protein variants of mutated isoform A depending on the splice acceptor site used; consensus acceptor site and alternative acceptor sites I or II. At the bottom, isoform D (A6NK88, encoded by ENST00000380725.1=CDKN1C-201, with a reading frame different from isoforms A and B) and the mutated isoform D (hybrid isoform D–A/B), consensus acceptor site used. The colours correspond to regions in figures 1 and 3, where intron sequences are written in lowercase letters and exon sequence in capital letters. The five deleted nucleotides are in green. The six inserted nucleotides in the mutated (delins) sequences are shown in red, and the out-of-frame sequence marked in blue. † denotes a predicted transcript that was not found on RNA sequencing.

the boy and grandfather, but not the mother, while expression in fibroblast was very low in the boy and undetectable in others. Results from cDNA sequencing and qPCR are not shown.

NGS-based cDNA sequencing

Ultra-deep RNA-seq was done for a more quantitative non-biased analysis of all transcripts, including the delins variant. The results are illustrated in figure 5. In summary, the analysis confirmed that the level of delins was 40%–50% in the boy (higher in fibroblast than in blood), 25% in the mosaic grandfather and 6% in the mother; that activation of alternative acceptor site I occurred in the boy's fibroblasts; and that *CDKN1C-201* represented 16%–42% of the total *CDKN1C* mRNA reads but accounted for the majority of the delins reads. Neither standard nor ultra-deep RNA sequencing could verify the presence of a predicted fifth transcript *CDKN1C-206* (ENST00000647251.1) that encodes a putative 175 aa protein product labelled isoform C (CCDS86169.1).

All RNA-seq samples had in total >340 million reads after filtering, and the numbers of *CDKN1C* tracks spanning splice junctions (SJTs) were between 35 and 204 (figure 5A). Visualisation of the alignment to NCBI Build 38 is presented with the counting of SJTs (online supplemental file). No delins reads were mapped against Build 38, and we suspected mapping problems. We then created three new FASTA reference files with the delins for accurate mapping (online supplemental file), one based on the consensus splice site and two with alternative acceptor sites I and II. Alignment to one of these putative delins splice sites unmasked the delins-specific tracks, while the other two alignments did not add more data and were therefore not further analysed. Figure 5A shows the result from the mapping of transcripts *CDKN1C-202, CDKN1C-203, CDKN1C-204* (combined) and *CDKN1C-201* against the reference sequence (green columns), and the distribution was compared with the sum of other *CDKN1C* transcripts. Likewise, the pink columns show the distribution of delins-mapped reads. The total distribution of delins and *CDKN1C-201* is also presented. SJTs presented as arcs in IGV (online supplemental file) showed that the vast majority of expressed transcripts have splicing from 5′-UTRs of different lengths, including *CDKN1C-201* and *CDKN1C-204*, and both use the alternative Met11 amino acid downstream and have four exons. In contrast, *CDKN1C-202* and *CDKN1C-203* always start at Met1 and have three exons. *CDKN1C-203* uses an alternative acceptor splice site five nucleotides downstream in the last exon and can be distinguished from other transcripts. The coding part of *CDKN1C-201* continues into exon 4, while this exon is making a 3′-UTR in other transcripts.

DISCUSSION

This family, where the index case has a mixture of diametrically opposed growth-related syndromes due to the same delins variant in *CDKN1C*, illustrates that the biological complexity of this small gene goes far beyond imprinting. Due to intricate gene splicing with frameshifting, this delins has an LoF effect on some isoforms and GoF effect on another. The latter is unexpected for a five against six nucleotides exchange and is due to the creation of a new splice acceptor site two nucleotides downstream of the canonical AG. Furthermore, we demonstrate that an alternative isoform with a different C-terminal reading frame (that we call isoform D, corresponding to transcript *CDKN1C-201*) is also affected, which turns the C terminus of isoform D back to the isoform A/B reading frame. If the hybrid D–A/B isoform transcript is expressed in the brain, this could be the cause of his developmental delay.

The asymptomatic carrier mother expressed the delins at a low level, as expected for a leaky paternally imprinted allele. The maternal grandfather was mosaic for the delins on his maternal allele, in agreement with an intermediate expression level. As a cautious note, the relative levels of the transcripts are not indicative of the degree of imprinting due to variable and poor expression, also affected by presumably inconsistent and non-uniform NMD. Variation in NMD efficiency within mRNA with the same PTC and subpopulations of mRNA escaping decay are reported, and this can contribute to explaining variation between individuals and between different tissues.[31 32]

Ultra-deep RNA sequencing proved to be superior to conventional RNA analysis, particularly on fibroblast RNA. Such unbiased sequencing verified the use of alternative acceptor site I and

A

	Map: Ref seq Build 38; wt SJT ex 2-3			Map: FASTA file with delins; delins SJT ex 2-3				% delins	% Iso D	
		CDKN1C-202,203,204 Iso A+B	*CDKN1C-201* Iso D		*CDKN1C-202,203,204* Iso A+B	*CDKN1C-201* Iso D	Alt.I AC Iso A+B			Total reads passing filter
	Total Wt	% (reads)	% (reads)	Total delins	% (reads)	% (reads)	% (reads)	% (delins/total)	% (isoD/IsoABD)	
Patient –Bl	62	77.4% (48)	22.6% (14)	43	30.2% (13)	69.8% (30)	-	41.0% (43/105)	41.9% (44/105)	476,053,970
Control-Bl	45	84.4% (38)	15.6% (7)	-	-	-	-	0% (0/45)	15.6% (7/45)	371,783,318
Mother-Bl	33	60.6% (20)	39.4% (13)	2	50% (1)	50% (1)	-	5.7% (2/35)	40.0% (14/35)	379,826,523
Grandfather-Bl	58	72.4% (42)	27.6% (16)	20	20% (4)	80% (16)	-	25.6% (20/78)	41.0% (32/78)	340,350,007
Patient-Fibr	92	66.3% (61)	33.7% (31)	112	44.6% (50)	44.6% (50)	10.7% (12)	54.9% (112/204)	39.7% (81/204)	340,350,007

B

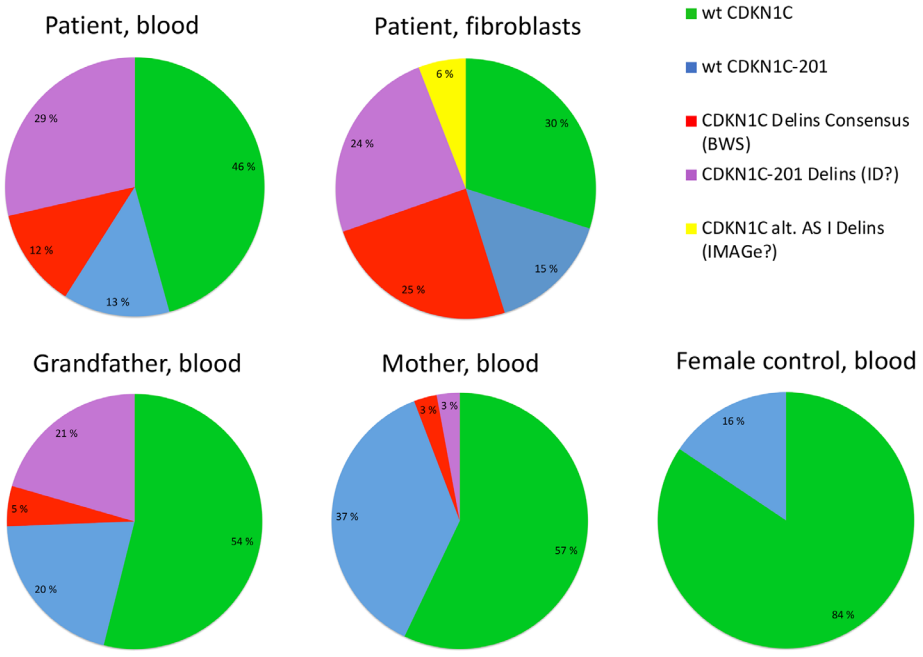

Figure 5 Result from NGS-based cDNA sequencing. (A) The number of reads spanning exon junctions (splice junction tracks, SJTs) after mapping to the reference sequence (from Genome Build 38, green background) and the delins-containing sequence (manually designed reference sequence, pink background). Reads with delins are shown in red. All reads were manually checked, and only SJTs spanning exons 2–3 are counted. Numbers are derived from figures as in the last part of the online supplemental file 1. Of note, reference sequence mapping did not detect any delins reads, probably because they were filtered out due to the complexity of the delins variant. (B) Sector diagrams illustrating the distributions of documented transcripts from RNA sequencing of RNA derived from blood samples and fibroblast. The percentages are calculated from the numbers in figure 5A. It was not possible to discriminate all *CDKN1C* transcripts by RNA sequencing, so *CDKN1C-202, CDKN1C-203* and *CDKN1C-204* are collectively referred to as *CDKN1C* in this figure, but *CDKN1C-201* transcripts (isoform D, UniProt: A6NK88) are identified. Green and blue colours represent wt reads of *CDKN1C* and *CDKN1C-201*, respectively, and red and purple colours represent delins reads using the consensus acceptor site in *CDKN1C* and *CDKN1C-201*, respectively. A fifth transcript (yellow) with delins *CDKN1C* using alternative acceptor site I, p.(Asp274GlufsTer47), was only documented in RNA from fibroblasts in the boy. The predicted or hypothetical clinical consequences of each of the four different mutated transcripts are noted in parentheses.

enabled us to quantify the expression of different transcripts, which again suggested which isoforms were most abundant. RNA sequencing as a first choice in a diagnostic pipeline would have been unsuccessful in this family as the delins could not be mapped with a single track against the reference sequence, but we solved this by mapping against dedicated reference files.

In summary, the boy fulfilled the clinical criteria of BWS—an overgrowth condition—despite being rather small and microcephalic, with a total score of 8, with two cardinal features (omphalocele and macroglossia) and four suggestive features (see table 1).[6] Macrosomia or neonatal overgrowth is common in BWS but is considered a suggestive and not a cardinal feature. There is no clinical consensus for IMAGe, but many of his non-BWS features overlap with this diagnosis. Adrenal insufficiency was never confirmed, but a mild and transient neonatal insufficiency could have been masked by continuous intravenous treatment of a leaking omphalocele. Genital abnormalities are described in both IMAGe and BWS, but small testes in IMAGe only.[22] Even though the renal size is not discussed in IMAGe (only fetal renal cortex size), his renal hypoplasia could very well be an IMAGe mirror of renal hyperplasia in BWS. Skeletal abnormalities are important findings in IMAGe, but besides asymmetry less important in SRS and are not features of BWS. Clinically, he did not pass the Netchine-Harbinson SRS score, having 3/6 criteria which is below the 4/6 limit.[33] His being small for gestational age, feeding difficulties, mild skeletal abnormalities and small testis are compatible with IMAGe, but this diagnosis is not definite as adrenal hypoplasia and metaphyseal

dysplasia were not documented. The clinical findings point to dual molecular effects with both LoF (BWS) and GoF (IMAGe) in CDKN1C. The latter can be explained by p.Asp274_276delinsAlaVal encoding transcript from alternative acceptor site II, but we could not confirm expression of this transcript in the two tissues tested. Another hypothetical GoF candidate is the p.Asp274GlufsTer47 encoding transcript from alternative acceptor site I with a verified GoF substitution Phe276Ser.[4] This transcript encodes an alternative C-terminal abolishing the PCNA-binding site, but the product might also be non-functional or degraded. Probably NMD is inefficient as a protective mechanism in *CDKN1C* as the truncated transcript from the consensus splice site, that is, encoding p.Asp274GlufsTer12 which is well within theoretical criteria for NMD, was present in both blood and fibroblasts.[34] This mutant product also substitutes IMAGe-related amino acids (figure 3) and might also have GoF effects.

A combination of opposing phenotypes due to a single mutation in the same gene is not reported earlier for *CDKN1C*, but for *GNAS*, another imprinted gene, this is not new.[35] Other genes where a variant is reported to cause both GoF and LoF effects are *RET*, *FLNA*, *GDF5* and *SMCHD1*.[36–39] In general, multinucleotide variants are potentially more damaging than single-nucleotide variants, illustrated by our family.[40]

The most intriguing finding was that the delins also affected a hitherto not confirmed transcript using a non-canonical reading frame—*CDKN1C-201*—which represented ~40% of all *CDKN1C* transcripts in the family (figure 5A). In contrast to wt *CDKN1C-201*, delins-mutated *CDKN1C-201* used the canonical reading frame, resulting in a hybrid D–A/B product that may be the cause of the unusual features in the boy. Alternative non-canonical reading frames are common in prokaryote and mitochondrial genes, but less so in eukaryotic and human genes, and another cell-cycle inhibitor gene, *CDKN2A*, is perhaps the most known example. This gene encodes at least two different proteins from different reading frames, p16(INK4) and p14(ARF). Both of these have splice variants, p16-gamma and p12, respectively, with tissue-specific expression.[41 42] Maybe this kind of regulatory complexity is a peculiarity of cyclin-dependent kinase inhibitors.

Our study identifies *CDKN1C-204* (isoform B) as the most abundant transcript, followed by *CDKN1C-201* (isoform D). The GTEx portal (gtexporal.org) suggests *CDKN1C-201* to be the most abundant isoform, particularly in the brain, followed by the isoforms encoded from *CDKN1C-204* and *CDKN1C-202*, but this could be explained by poor coverage of the PAPA-repeat region not included in the *CDKN1C-201*, that is, be artefactual. *CDKN1C-201* is only reported in humans and some higher primates.

Despite high *CDKN1C* expression in the embryonic brain, developmental delay and microcephaly are not considered features of either BWS or IMAGe, although brain abnormalities are reported in some patients.[7 11 43] However, behavioural and emotional difficulties and autistic spectrum disorders were found to be more frequent in BWS than controls, especially among patients with IC2 defects.[44] Moreover, in a cancer predisposition syndrome clinic, half of the patients with BWS or isolated hemihypertrophy needed special therapy.[45] Protein studies in embryonic brains of mice and rats suggested that Cdkn1c regulated newly formed migrating neurons,[46] and played a CDI-independent role in the maturation of midbrain dopaminergic neurons.[47] Differential spatial and temporal Cdkn1c expression in embryonic brain could be important for neurogenesis and gliogenesis, differentiation and generation of adult neural stem cells.[48–50] During cortical development, the differentiation of projection neurons was regulated via Cdkn1c.[51] According to a recent study, increased neuronal Cdkn1 expression resulted in abnormal social behaviour, implying that tightly regulated monoallelic expression is beneficial for neurological function.[52] Unexpectedly, brain-specific conditional deletion of the imprinted paternal *cdk1c* allele in mice resulted in microcephaly and thinning of the neocortex, despite low paternal expression (1%–2% of maternal levels) in control brains.[53]

The delins-mutated hybrid D–A/B transcript is our best explanation for the child's developmental delay. Brain damage due to neonatal hypoglycaemia or an untreated adrenal crisis was highly unlikely, and his brain MRI was normal, but prematurity and long hospitalisation might be contributing factors. Comparison with other IMAGe patients is difficult as many are not molecularly confirmed and could include phenocopies like MIRAGE syndrome.[54] Neither a high-resolution CNV analysis nor a trio-WES revealed alternative explanations for his developmental delay, but this cannot be excluded before further similar cases confirm a neurological association to *CDKN1C-201*. We searched the literature for other variants that may affect *CDKN1C-201* and came across a BWS family with a variant c.821–9C>A with an unknown function.[7] Unfortunately, no RNA was available to check the molecular consequence (Brioude, personal communication).

In summary, our findings demonstrate that a single delins variant can give rise to three distinct phenotypes through different molecular pathomechanisms. A hitherto not reported transcript *CDKN1C-201*, encoding an isoform D (A6NK88) with abundant brain expression, is also affected by the variant. Further functional studies or additional patients are needed to address the role of isoform D in brain development and to verify if changes to this isoform may cause a third face of the *CDKN1C* spectrum: developmental delay.

Acknowledgements We are most grateful to the family whose enthusiastic collaboration was essential to do such a complex genetic study. We also want to thank our coworkers Rita Holdhus, Hilde Rusaas, Guri Matre, Sigrid Erdal, Lene F Sandvik and Tomasz Stokowy. We also acknowledge the service from the Genomic Core Facility (GCF) at the University of Bergen, which is supported by Trond Mohn Foundation, for promoting the RNA sequencing.

Contributors SB has written and planned the article, and investigated the patients. BIH has planned and performed the molecular investigations. PBJ has contributed to the evaluation of the patient. GH has contributed to the planning and reviewing of the work.

Funding The authors have not declared a specific grant for this research from any funding agency in the public, commercial or not-for-profit sectors.

Competing interests None declared.

Patient consent for publication Parental/guardian consent obtained.

Provenance and peer review Not commissioned; externally peer reviewed.

Data availability statement All data relevant to the study are included in the article or uploaded as online supplemental information.

ORCID iD

Siren Berland http://orcid.org/0000-0002-8048-6682

REFERENCES

1 Eggermann T, Binder G, Brioude F, Maher ER, Lapunzina P, Cubellis MV, Bergadá I, Prawitt D, Begemann M. CDKN1C mutations: two sides of the same coin. *Trends Mol Med* 2014;20:614–22.
2 Hatada I, Ohashi H, Fukushima Y, Kaneko Y, Inoue M, Komoto Y, Okada A, Ohishi S, Nabetani A, Morisaki H, Nakayama M, Niikawa N, Mukai T. An imprinted gene p57KIP2 is mutated in Beckwith-Wiedemann syndrome. *Nat Genet* 1996;14:171–3.
3 Brioude F, Lacoste A, Netchine I, Vazquez M-P, Auber F, Audry G, Gauthier-Villars M, Brugieres L, Gicquel C, Le Bouc Y, Rossignol S. Beckwith-Wiedemann syndrome: growth pattern and tumor risk according to molecular mechanism, and guidelines for tumor surveillance. *Horm Res Paediatr* 2013;80:457–65.
4 Arboleda VA, Lee H, Parnaik R, Fleming A, Banerjee A, Ferraz-de-Souza B, Délot EC, Rodriguez-Fernandez IA, Braslavsky D, Bergadá I, Dell'Angelica EC, Nelson SF, Martinez-Agosto JA, Achermann JC, Vilain E. Mutations in the PCNA-binding domain of CDKN1C cause IMAGe syndrome. *Nat Genet* 2012;44:788–92.
5 Weksberg R, Shuman C, Beckwith JB. Beckwith-Wiedemann syndrome. *Eur J Hum Genet* 2010;18:8–14.
6 Brioude F, Kalish JM, Mussa A, Foster AC, Bliek J, Ferrero GB, Boonen SE, Cole T, Baker R, Bertoletti M, Cocchi G, Coze C, De Pellegrin M, Hussain K, Ibrahim A, Kilby MD, Krajewska-Walasek M, Kratz CP, Ladusans EJ, Lapunzina P, Le Bouc Y, Maas SM, Macdonald F, Õunap K, Peruzzi L, Rossignol S, Russo S, Shipster C, Skórka A, Tatton-Brown K, Tenorio J, Tortora C, Grønskov K, Netchine I, Hennekam RC, Prawitt D, Tümer Z, Eggermann T, Mackay DJG, Riccio A, Maher ER. Expert consensus document: clinical and molecular diagnosis, screening and management of Beckwith-Wiedemann syndrome: an international consensus statement. *Nat Rev Endocrinol* 2018;14:229–49.
7 Brioude F, Netchine I, Praz F, Le Jule M, Calmel C, Lacombe D, Edery P, Catala M, Odent S, Isidor B, Lyonnet S, Sigaudy S, Leheup B, Audebert-Bellanger S, Burglen L, Giuliano F, Alessandri J-L, Cormier-Daire V, Laffargue F, Blesson S, Coupier I, Lespinasse J, Blanchet P, Boute O, Baumann C, Polak M, Doray B, Verloes A, Viot G, Le Bouc Y, Rossignol S. Mutations of the imprinted CDKN1C gene as a cause of the overgrowth Beckwith-Wiedemann syndrome: clinical spectrum and functional characterization. *Hum Mutat* 2015;36:894–902.
8 Mussa A, Russo S, De Crescenzo A, Freschi A, Calzari L, Maitz S, Macchiaiolo M, Molinatto C, Baldassarre G, Mariani M, Tarani L, Bedeschi MF, Milani D, Melis D, Bartuli A, Cubellis MV, Selicorni A, Cirillo Silengo M, Larizza L, Riccio A, Ferrero GB. (Epi)genotype-phenotype correlations in Beckwith-Wiedemann syndrome. *Eur J Hum Genet* 2016;24:183–90.
9 Welsh HI, Stockley TL, Parkinson N, Ardinger HH. CDKN1C mutations and genital anomalies. *Am J Med Genet A* 2012;158A:265.
10 Romanelli V, Belinchón A, Benito-Sanz S, Martínez-Glez V, Gracia-Bouthelier R, Heath KE, Campos-Barros A, García-Miñaur S, Fernandez L, Meneses H, López-Siguero JP, Guillén-Navarro E, Gómez-Puertas P, Wesselink J-J, Mercado G, Esteban-Marfil V, Palomo R, Mena R, Sánchez A, Del Campo M, Lapunzina P. CDKN1C (p57(Kip2)) analysis in Beckwith-Wiedemann syndrome (BWS) patients: genotype–phenotype correlations, novel mutations, and polymorphisms. *Am J Med Genet A* 2010;152A:1390–7.
11 Gardiner K, Chitayat D, Choufani S, Shuman C, Blaser S, Terespolsky D, Farrell S, Reiss R, Wodak S, Pu S, Ray PN, Baskin B, Weksberg R. Brain abnormalities in patients with Beckwith-Wiedemann syndrome. *Am J Med Genet A* 2012;158A:1388–94.
12 Jurkiewicz D, Skórka A, Ciara E, Kugaudo M, Pelc M, Chrzanowska K, Krajewska-Walasek M. Rare clinical findings in three sporadic cases of Beckwith-Wiedemann syndrome due to novel mutations in the CDKN1C gene. *Clin Dysmorphol* 2020;29:28–34.
13 Brioude F, Oliver-Petit I, Blaise A, Praz F, Rossignol S, Le Jule M, Thibaud N, Faussat A-M, Tauber M, Le Bouc Y, Netchine I. CDKN1C mutation affecting the PCNA-binding domain as a cause of familial Russell Silver syndrome. *J Med Genet* 2013;50:823–30.
14 Kerns SL, Guevara-Aguirre J, Andrew S, Geng J, Guevara C, Guevara-Aguirre M, Guo M, Oddoux C, Shen Y, Zurita A, Rosenfeld RG, Ostrer H, Hwa V, Dauber A. A novel variant in CDKN1C is associated with intrauterine growth restriction, short stature, and early-adulthood-onset diabetes. *J Clin Endocrinol Metab* 2014;99:E2117–22.
15 Obermann C, Meyer E, Prager S, Tomiuk J, Wollmann HA, Eggermann T. Searching for genomic variants in IGF2 and CDKN1C in Silver-Russell syndrome patients. *Mol Genet Metab* 2004;82:246–50.
16 Suntharalingham JP, Ishida M, Buonocore F, Del Valle I, Solanky N, Demetriou C, Regan L, Moore GE, Achermann JC. Analysis of *CDKN1C* in fetal growth restriction and pregnancy loss. *F1000Res* 2019;8.
17 Inoue T, Nakamura A, Iwahashi-Odano M, Tanase-Nakao K, Matsubara K, Nishioka J, Maruo Y, Hasegawa Y, Suzumura H, Sato S, Kobayashi Y, Murakami N, Nakabayashi K, Yamazawa K, Fuke T, Narumi S, Oka A, Ogata T, Fukami M, Kagami M. Contribution of gene mutations to Silver-Russell syndrome phenotype: multigene sequencing analysis in 92 etiology-unknown patients. *Clin Epigenetics* 2020;12:86.
18 Vilain E, Le Merrer M, Lecointre C, Desangles F, Kay MA, Maroteaux P, McCabe ER. IMAGe, a new clinical association of intrauterine growth retardation, metaphyseal dysplasia, adrenal hypoplasia congenita, and genital anomalies. *J Clin Endocrinol Metab* 1999;84:4335–40.
19 Heide S, Chantot-Bastaraud S, Keren B, Harbison MD, Azzi S, Rossignol S, Michot C, Lackmy-Port Lys M, Demeer B, Heinrichs C, Newfield RS, Sarda P, Van Maldergem L, Trifard V, Giabicani E, Siffroi J-P, Le Bouc Y, Netchine I, Brioude F. Chromosomal rearrangements in the 11p15 imprinted region: 17 new 11p15.5 duplications with associated phenotypes and putative functional consequences. *J Med Genet* 2018;55:205–13.
20 Hamajima N, Johmura Y, Suzuki S, Nakanishi M, Saitoh S. Increased protein stability of CDKN1C causes a gain-of-function phenotype in patients with IMAGe syndrome. *PLoS One* 2013;8:e75137.
21 Bodian DL, Solomon BD, Khromykh A, Thach DC, Iyer RK, Link K, Baker RL, Baveja R, Vockley JG, Niederhuber JE. Diagnosis of an imprinted-gene syndrome by a novel bioinformatics analysis of whole-genome sequences from a family trio. *Mol Genet Genomic Med* 2014;2:530–8.
22 Kato F, Hamajima T, Hasegawa T, Amano N, Horikawa R, Nishimura G, Nakashima S, Fuke T, Sano S, Fukami M, Ogata T. IMAGe syndrome: clinical and genetic implications based on investigations in three Japanese patients. *Clin Endocrinol* 2014;80:706–13.
23 Homma TK, Freire BL, Honjo Kawahira RS, Dauber A, Funari MFdeA, Lerario AM, Nishi MY, Albuquerque EVde, Vasques GdeA, Collett-Solberg PF, Miura Sugayama SM, Bertola DR, Kim CA, Arnhold IJP, Malaquias AC, Jorge AAdeL. Genetic disorders in prenatal onset syndromic short stature identified by exome sequencing. *J Pediatr* 2019;215:192–8.
24 Sabir AH, Ryan G, Mohammed Z, Kirk J, Kiely N, Thyagarajan M, Cole T. Familial Russell-Silver syndrome like phenotype in the PCNA domain of the *CDKN1C* gene, a further case. *Case Rep Genet* 2019;2019:1–8.
25 Binder G, Ziegler J, Schweizer R, Habhab W, Haack TB, Heinrich T, Eggermann T. Novel mutation points to a hot spot in CDKN1C causing Silver-Russell syndrome. *Clin Epigenetics* 2020;12:152.
26 Borges KS, Arboleda VA, Vilain E. Mutations in the PCNA-binding site of CDKN1C inhibit cell proliferation by impairing the entry into S phase. *Cell Div* 2015;10:2.
27 Balasubramanian M, Sprigg A, Johnson DS. IMAGe syndrome: case report with a previously unreported feature and review of published literature. *Am J Med Genet A* 2010;152A:3138–42.
28 Kim D, Langmead B, Salzberg SL. HISAT: a fast spliced aligner with low memory requirements. *Nat Methods* 2015;12:357–60.
29 Pertea M, Kim D, Pertea GM, Leek JT, Salzberg SL. Transcript-level expression analysis of RNA-seq experiments with HISAT, StringTie and Ballgown. *Nat Protoc* 2016;11:1650–67.
30 Liao Y, Smyth GK, Shi W. featureCounts: an efficient general purpose program for assigning sequence reads to genomic features. *Bioinformatics* 2014;30:923–30.
31 Hoek TA, Khuperkar D, Lindeboom RGH, Sonneveld S, Verhagen BMP, Boersma S, Vermeulen M, Tanenbaum ME. Single-molecule imaging uncovers rules governing nonsense-mediated mRNA decay. *Mol Cell* 2019;75:e11:324–39.
32 Nguyen LS, Wilkinson MF, Gecz J. Nonsense-mediated mRNA decay: inter-individual variability and human disease. *Neurosci Biobehav Rev* 2014;46 Pt 2:175–86.
33 Wakeling EL, Brioude F, Lokulo-Sodipe O, O'Connell SM, Salem J, Bliek J, Canton APM, Chrzanowska KH, Davies JH, Dias RP, Dubern B, Elbracht M, Giabicani E, Grimberg A, Grønskov K, Hokken-Koelega ACS, Jorge AA, Kagami M, Linglart A, Maghnie M, Mohnike K, Monk D, Moore GE, Murray PG, Ogata T, Petit IO, Russo S, Said E, Toumba M, Tümer Z, Binder G, Eggermann T, Harbison MD, Temple IK, Mackay DJG, Netchine I. Diagnosis and management of Silver-Russell syndrome: first international consensus statement. *Nat Rev Endocrinol* 2017;13:105–24.
34 Fatscher T, Boehm V, Gehring NH, Mechanism GNH. Mechanism, factors, and physiological role of nonsense-mediated mRNA decay. *Cell Mol Life Sci* 2015;72:4523–44.
35 Iiri T, Herzmark P, Nakamoto JM, van Dop C, Bourne HR. Rapid GDP release from Gs alpha in patients with gain and loss of endocrine function. *Nature* 1994;371:164–8.
36 Decker RA, Peacock ML. Occurrence of MEN 2a in familial Hirschsprung's disease: a new indication for genetic testing of the RET proto-oncogene. *J Pediatr Surg* 1998;33:207–14.
37 Zenker M, Rauch A, Winterpacht A, Tagariello A, Kraus C, Rupprecht T, Sticht H, Reis A. A dual phenotype of periventricular nodular heterotopia and frontometaphyseal dysplasia in one patient caused by a single FLNA mutation leading to two functionally different aberrant transcripts. *Am J Hum Genet* 2004;74:731–7.
38 Degenkolbe E, König J, Zimmer J, Walther M, Reißner C, Nickel J, Plöger F, Raspopovic J, Sharpe J, Dathe K, Hecht JT, Mundlos S, Doelken SC, Seemann P. A GDF5 point mutation strikes twice—causing BDA1 and SYNS2. *PLoS Genet* 2013;9:e1003846.
39 Shaw ND, Brand H, Kupchinsky ZA, Bengani H, Plummer L, Jones TI, Erdin S, Williamson KA, Rainger J, Stortchevoi A, Samocha K, Currall BB, Dunican DS, Collins RL, Willer JR, Lek A, Lek M, Nassan M, Pereira S, Kammin T, Lucente D, Silva A, Seabra CM, Chiang C, An Y, Ansari M, Rainger JK, Joss S, Smith JC, Lippincott MF, Singh SS, Patel N, Jing JW, Law JR, Ferraro N, Verloes A, Rauch A, Steindl K, Zweier M, Scheer I, Sato D, Okamoto N, Jacobsen C, Tryggestad J, Chernausek S, Schimmenti LA, Brasseur B, Cesaretti C, García-Ortiz JE, Buitrago TP, Silva OP, Hoffman JD, Mühlbauer W, Ruprecht KW, Loeys BL, Shino M, Kaindl AM, Cho C-H, Morton CC, Meehan RR, van Heyningen V, Liao EC, Balasubramanian R, Hall JE, Seminara SB, Macarthur D, Moore SA, Yoshiura K-I, Gusella JF, Marsh JA, Graham JM, Lin AE, Katsanis N, Jones PL, Crowley WF, Davis EE, FitzPatrick DR, Talkowski ME. Smchd1 mutations associated

with a rare muscular dystrophy can also cause isolated arhinia and Bosma arhinia microphthalmia syndrome. *Nat Genet* 2017;49:238–48.
40 Kaplanis J, Akawi N, Gallone G, McRae JF, Prigmore E, Wright CF, Fitzpatrick DR, Firth HV, Barrett JC, Hurles ME, Deciphering Developmental Disorders study. Exome-wide assessment of the functional impact and pathogenicity of multinucleotide mutations. *Genome Res* 2019;29:1047–56.
41 Robertson KD, Jones PA. Tissue-specific alternative splicing in the human INK4a/ARF cell cycle regulatory locus. *Oncogene* 1999;18:3810–20.
42 Lin Y-C, Diccianni MB, Kim Y, Lin H-H, Lee C-H, Lin R-J, Joo SH, Li J, Chuang T-J, Yang A-S, Kuo H-H, Tsai M-D, Yu AL. Human p16gamma, a novel transcriptional variant of p16(INK4A), coexpresses with p16(INK4A) in cancer cells and inhibits cell-cycle progression. *Oncogene* 2007;26:7017–27.
43 Udayakumaran S, Onyia CU. Beckwith-Wiedemann syndrome and Chiari I malformation—a case-based review of central nervous system involvement in hemihypertrophy syndromes. *Childs Nerv Syst* 2015;31:637–41.
44 Kent L, Bowdin S, Kirby GA, Cooper WN, Maher ER. Beckwith Weidemann syndrome: a behavioral phenotype–genotype study. *Am J Med Genet B Neuropsychiatr Genet* 2008;147B:1295–7.
45 Groves AP, Gettinger K, Druley TE, Kozel BA, Shinawi M, Mohrmann C, Henry J, Jacobi C, Trinkaus K, Hayashi RJ. Special therapy and psychosocial needs identified in a multidisciplinary cancer predisposition syndrome clinic. *J Pediatr Hematol Oncol* 2019;41:133–6.
46 Itoh Y, Masuyama N, Nakayama K, Nakayama KI, Gotoh Y. The cyclin-dependent kinase inhibitors p57 and p27 regulate neuronal migration in the developing mouse neocortex. *J Biol Chem* 2007;282:390–6.
47 Joseph B, Wallén-Mackenzie A, Benoit G, Murata T, Joodmardi E, Okret S, Perlmann T. p57(Kip2) cooperates with Nurr1 in developing dopamine cells. *Proc Natl Acad Sci U S A* 2003;100:15619–24.
48 Ye W, Mairet-Coello G, Pasoreck E, Dicicco-Bloom E. Patterns of p57Kip2 expression in embryonic rat brain suggest roles in progenitor cell cycle exit and neuronal differentiation. *Dev Neurobiol* 2009;69:1–21.
49 Tury A, Mairet-Coello G, DiCicco-Bloom E. The cyclin-dependent kinase inhibitor p57Kip2 regulates cell cycle exit, differentiation, and migration of embryonic cerebral cortical precursors. *Cereb Cortex* 2011;21:1840–56.
50 Furutachi S, Miya H, Watanabe T, Kawai H, Yamasaki N, Harada Y, Imayoshi I, Nelson M, Nakayama KI, Hirabayashi Y, Gotoh Y. Slowly dividing neural progenitors are an embryonic origin of adult neural stem cells. *Nat Neurosci* 2015;18:657–65.
51 Pfurr S, Chu Y-H, Bohrer C, Greulich F, Beattie R, Mammadzada K, Hils M, Arnold SJ, Taylor V, Schachtrup K, Uhlenhaut NH, Schachtrup C. The E2A splice variant E47 regulates the differentiation of projection neurons via p57(KIP2) during cortical development. *Development* 2017;144:3917–31.
52 McNamara GI, John RM, Isles AR. Territorial behavior and social stability in the mouse require correct expression of imprinted *Cdkn1c*. *Front Behav Neurosci* 2018;12:28.
53 Imaizumi Y, Furutachi S, Watanabe T, Miya H, Kawaguchi D, Gotoh Y. Role of the imprinted allele of the CDKN1C gene in mouse neocortical development. *Sci Rep* 2020;10:1884.
54 Kim Y-M, Seo GH, Kim G-H, Ko JM, Choi J-H, Yoo H-W. A case of an infant suspected as IMAGE syndrome who were finally diagnosed with MIRAGE syndrome by targeted Mendelian exome sequencing. *BMC Med Genet* 2018;19:35.